

Transplantation and *in vivo* imaging of multilineage engraftment in zebrafish bloodless mutants

David Traver¹, Barry H Paw¹, Kenneth D Poss², W Todd Penberthy³, Shuo Lin³ & Leonard I Zon¹

The zebrafish is firmly established as a genetic model for the study of vertebrate blood development. Here we have characterized the blood-forming system of adult zebrafish. Each major blood lineage can be isolated by flow cytometry, and with these lineal profiles, defects in zebrafish blood mutants can be quantified. We developed hematopoietic cell transplantation to study cell autonomy of mutant gene function and to establish a hematopoietic stem cell assay. Hematopoietic cell transplantation can rescue multilineage hematopoiesis in embryonic lethal *gata1*^{-/-} mutants for over 6 months. Direct visualization of fluorescent donor cells in embryonic recipients allows engraftment and homing events to be imaged in real time. These results provide a cellular context in which to study the genetics of hematopoiesis.

Hematopoietic stem cells (HSCs) exist as rare populations in blood-forming tissues that both self-renew and generate all blood cell lineages for the life of the host. It is now possible to prospectively isolate murine HSCs¹⁻³, clonogenic progenitors downstream of HSCs that give rise to all cells of the lymphoid⁴ and myeloerythroid⁵ lineages, and most mature blood lineages, by cell surface phenotype. This work has led to an understanding of the lineage relationships among all blood cell types and the stages through which each passes in its differentiation hierarchy. In contrast to what is known regarding the phylogeny of hematopoietic cells, the molecular mechanisms underlying stem cell specification, self-renewal, amplification and lineal fate decisions remain poorly understood.

Gene-disruption experiments in mice have shown absolute requirements for the function of genes such as *Tal1* (ref. 6), *Lmo2* (refs. 7,8), *Runx1* (ref. 9) and *Myb*¹⁰ in the development and/or maintenance of fetal HSCs. Microarray approaches have also been used to compare global gene expression profiles among prospectively isolated HSCs, committed progenitors and mature blood cell populations¹¹. Although both approaches can be powerful, neither is well suited for unbiased identification or high-throughput functional testing of candidate blood genes.

The zebrafish has emerged as a unique vertebrate model system for the analysis of developmental processes because of its larval transparency and high fecundity and the ease with which forward genetic and expression screens can demonstrate previously unknown genes in a relatively unbiased way¹². Large-scale mutagenesis screens have produced over 50 mutants in blood cell development that fall into at least 26 complementation groups^{13,14}. These mutants show defects in a wide range of hematopoietic processes, including HSC specification¹⁵⁻¹⁷,

lymphoid and thymic development¹⁸ and the generation of functional myeloid¹⁹ and erythroid^{13,14} cells.

Because of the early time points analyzed and the visual nature of these screens, most mutants have defects in the formation or maintenance of embryonic, also known as primitive, red blood cells. As with blood development in mammals, birds and frogs, zebrafish hematopoiesis occurs in several anatomic sites during embryogenesis and larval development²⁰. The first wave of hematopoiesis occurs in a structure called the intermediate cell mass that is similar to the mammalian yolk sac in that primitive erythrocytes are the main cell type produced. Later, hematopoiesis shifts to the ventral wall of the dorsal aorta, the zebrafish equivalent of the aorta-gonad-mesonephros region. Based on the expression of markers such as *cmyb*²¹ and *runx1* (refs. 22,23), it seems that the zebrafish aorta-gonad-mesonephros specifies HSCs with definitive, multilineage potential. At present, screens aimed at identifying HSC mutants due to alterations in these markers require systematic characterization of steady-state, definitive hematopoiesis and the development of tools to study HSC biology more precisely.

We have established several tools to characterize the definitive blood-forming system of adult zebrafish. With the ability to analyze and isolate each major blood cell lineage, we show that zebrafish embryonic blood mutants often demonstrate previously unrecognized defects as adults, even as heterozygous carriers of recessive mutations. Transplantation of adult kidney marrow into prethymic embryonic recipients generates long-term hematopoietic reconstitution of otherwise lethal *gata1*^{-/-} mutants in the apparent absence of graft-versus-host disease. Hematopoietic cell transplantation in zebrafish will thus allow future studies to measure HSC activity and to characterize

¹Children's Hospital Boston and the Howard Hughes Medical Institute, 320 Longwood Avenue, Enders 720, Boston, Massachusetts 02115, USA. ²Department of Cell Biology, Box 3709, Duke University Medical Center, Durham, North Carolina 27710, USA. ³University of California at Los Angeles, 621 Charles Young Drive South, LS4325, Los Angeles, California 90095, USA. Correspondence should be addressed to L.I.Z. (zon@rascal.med.harvard.edu).

Published online 9 November 2003; doi:10.1038/ni1007

Table 1 Differential cell counts in adult hematolymphoid organs

		<i>n</i>	Percentage of cells ^a						
			Blast	Neutrophil	Eosinophil	Monocyte Macrophage	Proerythrocyte Erythrocyte	Prothrombocyte Thrombocyte	Lymphocyte
Kidney	Manual	15	6.4 ± 2.0	11.8 ± 3.8	9.8 ± 2.8	6.8 ± 1.7	41.3 ± 9.3	2.0 ± 1.0	21.1 ± 5.2
	Flow	29	6.0 ± 1.9	Myelomonocytes 23.7 ± 5.7			40.6 ± 8.2	1.6 ± 0.4	19.2 ± 3.9
Spleen	Manual	14	<1	2.6 ± 1.3	3.3 ± 1.6	3.6 ± 1.8	72.5 ± 7.5	3.9 ± 1.1	13.2 ± 4.4
	Flow	16	<1	Myelomonocytes 2.6 ± 1.0			79.1 ± 4.2	4.2 ± 1.4	11.3 ± 2.5
Blood	Manual	5	<1	<1	<1	<1	99.2 ± 0.8	<1	<1
	Flow	11	<1	Myelomonocytes <1			97.6 ± 1.5	0.6 ± 0.1	1.0 ± 0.6
	NEC ^b	13	<1	3.3 ± 2.5	1.0 ± 0.9	3.1 ± 2.1	—	63.2 ± 10.0	30.0 ± 9.3

Numbers are presented as means, plus or minus standard deviations. Average WKM cell counts were $1.3 \pm 0.5 \times 10^6$ ($n = 16$), and splenocyte counts were $4.4 \pm 1.8 \times 10^5$ ($n = 15$). ND, no data. ^aDifferential cell counts were obtained by identifying at least 200 cells per kidney and spleen cytospin and 1,000 cells per blood smear. ^bNEC (non-erythroid compartment) is the percentage of manually counted blood leukocytes.

genetic defects in zebrafish blood mutants. Finally, the development of transgenic animals with red fluorescent erythrocytes and green fluorescent leukocytes has enabled, for the first time to our knowledge, direct visualization of early trafficking events in embryos and multilineage engraftment in adults in living transplant recipients.

RESULTS

Analysis of zebrafish hematolymphoid sites

Blood production in adult zebrafish, as in other teleosts, occurs in the kidney, which supports both renal functions and multilineage hematopoiesis²⁴. All mature blood cell types are found in the kidney, and they morphologically resemble their mammalian counterparts, with the exceptions that erythrocytes remain nucleated and thrombocytes perform the clotting functions of platelets²⁵. As determined by differential cell counts, the absence of immature precursors in other hematolymphoid tissues indicates that the kidney is the main hematopoietic site in adult zebrafish (Table 1). The dorsal aorta is intimately associated with the kidney and cannot be separately dissected. Our kidney counts and preparations thus reflect combined contributions from the kidney and aorta that we collectively call whole-kidney marrow (WKM).

Major blood lineages are isolatable by flow cytometry

Analysis of WKM by flow cytometry showed that several distinct populations could be resolved by light-scatter characteristics (Fig. 1). Forward

scatter (FSC) is directly proportional to cell size and side scatter (SSC) is proportional to cellular granularity²⁶. Using combined scatter profiles, we isolated the major blood lineages from WKM after two rounds of cell sorting. Mature erythroid cells were exclusively in a FSC^{lo} fraction. Myelomonocytic cells (including neutrophils, also known as heterophilic granulocytes, monocytes, macrophages and eosinophils, also known as eo/basophils) were only in a FSC^{hi}SSC^{hi} population, lymphoid cells were in a FSC^{int}SSC^{lo} subset and immature precursors were in a FSC^{hi}SSC^{int} subset (Fig. 1). Two distinct populations existed in the erythrocyte fraction (Fig. 1, red circled gate). Attempts at sorting either of these subsets reproducibly resulted in approximately equal recovery of both. This result is probably because of the elliptical nature of zebrafish red blood cells, as sorting of all other populations yielded cells that were in the original sorting gates after reanalysis. Using 2- μ m and 10- μ m latex beads, we determined the mean cell size of each scatter population. Precursor cells had a mean size of 13.8 μ m; myeloid cells, 15.2 μ m; erythroid cells, 6.2 μ m; and lymphoid cells, 8.3 μ m.

Examination of splenic and peripheral blood suspensions showed each had a profile distinct from that of WKM, being mainly erythroid (data not shown). Sorting of each scatter population from spleen and blood showed each contained only erythrocytes, lymphocytes or myelomonocytes (data not shown). We did not find immature precursors in either tissue. Percentages of cells in each scatter population closely matched those obtained by morphological cell counts in all

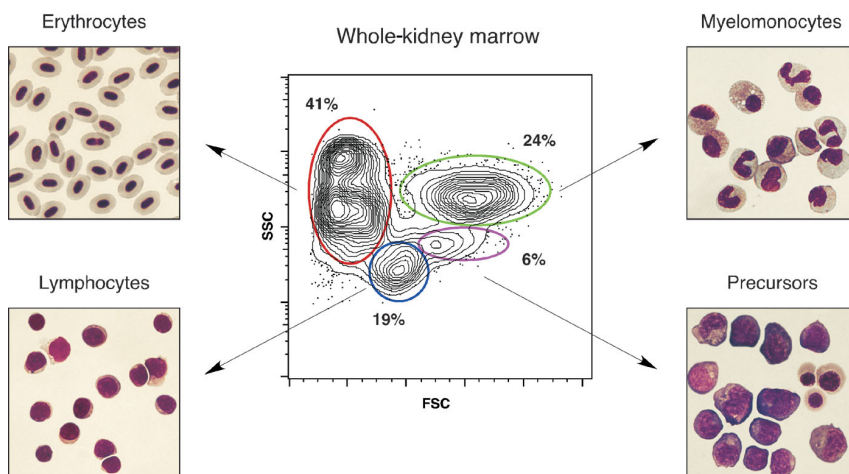


Figure 1 Separation of major blood cell lineages from WKM by light-scatter characteristics. FSC is directly proportional to cell size and SSC is indicative of cellular granularity. FSC^{lo} subsets are composed entirely of mature erythrocytes (red-outlined gate), FSC^{int}SSC^{lo} subsets are highly enriched for lymphocytes (blue-outlined gate), FSC^{hi}SSC^{int} subsets are composed of immature precursors of all lineages (purple-outlined gate) and FSC^{hi}SSC^{hi} subsets are composed only of mature myelomonocytic cells (green-outlined gate). Relative means of each scatter population were obtained from 29 adult zebrafish.

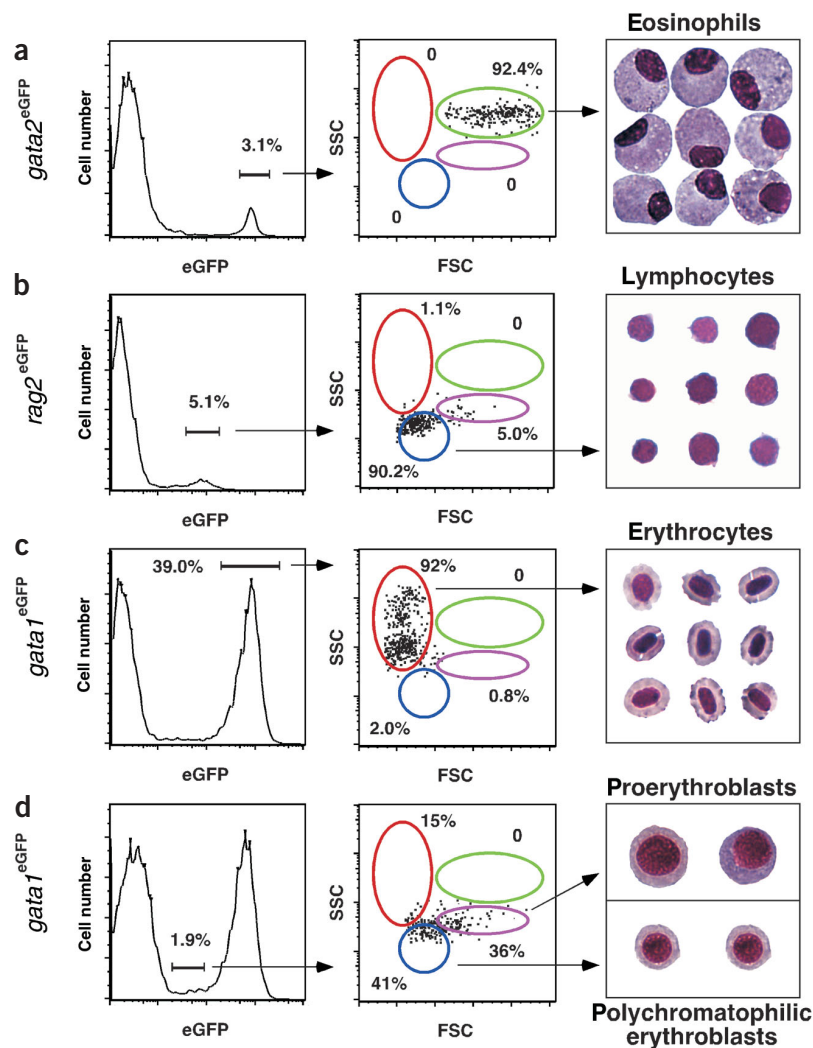


Figure 2 Analysis of zebrafish transgenic lines by flow cytometry. (a) Analysis of WKM cells marked by a *gata2*^{eGFP} transgene. GFP⁺ cells gated from the WKM histogram (left) were sorted and reanalyzed by forward and side scatter (middle). Nearly all cells are in the myeloid gate, and morphological analysis shows all cells are eosinophils (right). (b) Analysis of *rag2*^{eGFP} WKM shows that more than 90% of GFP⁺ cells are in the lymphoid fraction. All sorted cells show lymphoid morphologies (right). (c) Approximately 40% of WKM cells express a *gata1*^{eGFP} transgene. GFP^{hi} cells are in the FSC^{lo} erythroid scatter fraction. Morphological analysis shows all cells are terminally differentiated erythrocytes (right). (d) A minor population of cells in *gata1*^{eGFP} animals are GFP^{lo}. Right, double sorting of GATA-1^{lo} cells shows the precursor fraction is enriched for immature proerythroblasts (top), whereas the lymphoid fraction contains smaller polychromatophilic erythroblasts (bottom). Percents indicate relative percentages of GFP⁺ cells within WKM.

($n = 3$) of WKM cells were GFP⁺, and over 90% of this population localized in the lymphoid scatter fraction (FSC^{int}SSC^{lo}). Morphological analysis showed all cells had the characteristics of immature lymphocytes (Fig. 2b). Analysis of zebrafish with an erythroid-specific *gata1*^{eGFP} transgene²⁹ showed $39.0 \pm 5.9\%$ ($n = 3$) of WKM cells had high expression of GFP. Isolation of this subset showed that over 90% were in the erythroid scatter gate (FSC^{lo}), and all purified cells had the morphology of mature erythrocytes (Fig. 2c). The *gata1*^{eGFP} animals also had a rare population ($1.9 \pm 0.3\%$; $n = 3$) of GFP^{lo} cells. Isolation of this subset showed they were in the precursor, lymphoid and erythroid scatter fractions (Fig. 2d). Sorted GFP^{lo} cells all had immature erythroid morphologies,

tissues, demonstrating that this flow cytometric assay is accurate in measuring the relative percentages of each of the major blood lineages (Table 1). Thus, the kidney seems to be the main site of hematopoiesis in adult zebrafish.

Analysis of zebrafish transgenic lines by flow cytometry

Because we assigned the lineal designations for each kidney scatter population by morphology, we next assessed whether the expression of lineage-affiliated genes correlated with specific scatter fractions. We used transgenic zebrafish that express green fluorescent protein (GFP) under the control of lineage-specific gene promoters. GATA2 has been shown in mammalian studies to be expressed in both eosinophils and basophils²⁷. Analysis of WKM isolated from transgenic zebrafish expressing enhanced GFP under control of a *gata2* bacterial artificial chromosome construct (*gata2*^{eGFP}) showed that $3.1 \pm 1.0\%$ ($n = 3$) of WKM cells were GFP⁺. Sorting of this fraction showed nearly all cells were in the myeloid scatter fraction (FSC^{hi}SSC^{hi}), and morphological analysis showed all sorted cells had the morphological characteristics of eosinophils (Fig. 2a). Similar analysis of transgenic zebrafish expressing GFP under the control of the lymphoid-specific recombination-activating gene 2 (*rag2*) promoter²⁸ showed that $5.1 \pm 0.9\%$

ranging from early proerythroblasts to late polychromatophilic erythroblasts (Fig. 2d). GFP^{lo} cell populations sorted from the precursor fraction were enriched for the former cell type, whereas cell populations sorted from the lymphoid fraction were enriched for the latter, more mature cell types (Fig. 2d). These data indicate that the erythroid maturation pathway, in terms of kidney scatter populations, seems to transit from immature proerythroblasts in the precursor scatter fraction to maturing late erythroblasts adjacent to and partially in the lymphoid scatter fraction before their terminal differentiation and appearance in the erythroid gate. CD41, also known as platelet glycoprotein IIb and integrin α_{IIb} (gene name, *itga2b*), is specifically expressed on zebrafish thrombocytes; analysis of *itga2b*^{eGFP}-transgenic animals showed that rare prothrombocytes (CD41^{lo}, $0.8 \pm 0.3\%$ of WKM; $n = 27$) were in the precursor population, and that mature thrombocytes (CD41^{hi}, $0.8 \pm 0.4\%$ of WKM; $n = 27$) were in the lymphoid fraction (H.F. Lin, D.T., C. Abraham and R. Handin, unpublished data). The GATA-1^{lo} and CD41^{hi} cells account for approximately 10% of the cells in the lymphoid gate. Although relatively minor, these analyses show that the lymphoid scatter fraction, unlike the erythroid and myeloid fractions, contains precursors of other blood cell lineages.

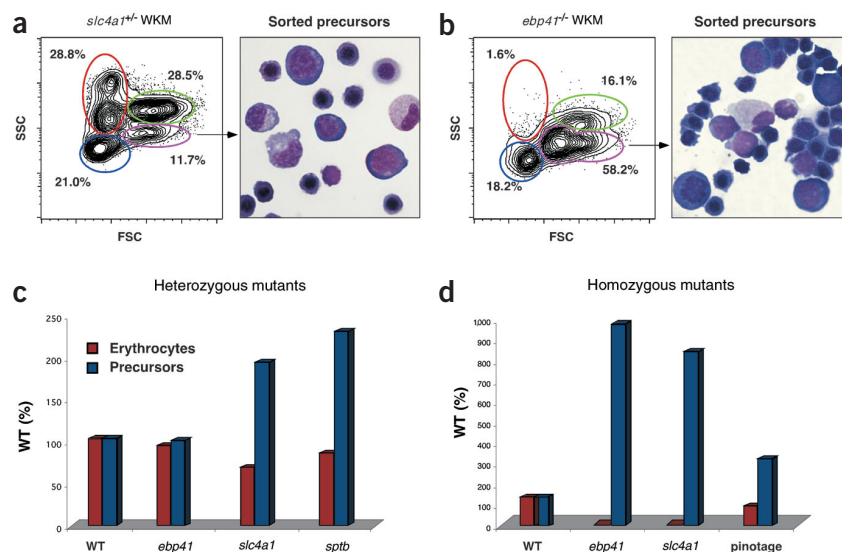


Figure 3 Flow cytometry profiling of zebrafish blood mutants. (a) Scatter profile of WKM in a typical *slc4a1* heterozygous mutant (left). Sorted precursors show a preponderance of immature erythroid elements (right). (b) WKM scatter profile of a typical *ebp41* homozygous mutant (left). Sorted precursors show nearly all cells are immature erythroid cells that range from proerythroblasts to late polychromatophilic erythroblasts (right). Numbers in plots in a and b indicate percent of cells in circled gate. (c) Comparison of mean percentages of WKM erythrocyte and precursor scatter populations among heterozygous blood mutants and wild-type (WT) controls. All mutant means (*ebp41*, $n = 18$; *slc4a1*, $n = 22$; *sptb*, $n = 8$) were normalized to wild-type means ($n = 29$), which were defined as 100%. (d) Relative means of homozygous blood mutants (*ebp41*, $n = 6$; *slc4a1*, $n = 3$; *pinotage*, $n = 9$) normalized to wild-type (WT) control values.

Characterization of zebrafish blood mutants by flow cytometry

To test whether flow cytometric profiling could serve as a diagnostic tool, we examined zebrafish blood mutants by flow cytometry (Fig. 3). Nearly all blood mutants identified so far have shown defects in embryonic erythrocytes¹². Most of these mutations are recessive, and many are embryonic lethal when homozygous. These mutants include merlot, retsina and riesling, which have defects in the genes encoding erythrocyte membrane protein band 4.1 (*epb41*)³⁰, solute carrier family 4, anion exchanger 1 (*slc4a1*)³¹ and erythrocytic β -spectrin (*sptb*)³², respectively. All three genes are expressed specifically in the erythrocyte membrane, and homozygous mutants show decreasing blood counts in the larval stages because of failures in membrane integrity. To determine whether heterozygous carriers of each mutation show adult hematopoietic deficiencies, we analyzed WKM suspensions by flow cytometry. Mutants heterozygous for the *epb41* mutation had percentages of erythroid and precursor cells similar to those of their wild-type siblings (Fig. 3c). Mutants heterozygous for the *slc4a1* mutation, however, showed mild anemia with a concomitant twofold increase in the precursor scatter population (Fig. 3a,c). Sorting of the precursor fraction showed a preponderance of immature erythroid cells (Fig. 3a). In contrast, enumeration of cell types from sorted wild-type precursor fractions showed approximately 40% myeloid precursors, 40% erythroid precursors and 20% lymphoid precursors by morphological criteria. The *sptb* mutant showed a similar heterozygous phenotype, with anemia associated with precursor increases (Fig. 3c). The phenotypes of both adult *slc4a1* and *sptb* heterozygotes seemed intermediate to those of their wild-type siblings and embryonic homozygous mutants. For example, *slc4a1*^{-/-} embryos die because of a block in erythropoiesis at the polychromatophilic erythroblast stage³¹. Adult *slc4a1*^{+/-} animals showed a partial but incomplete block at this stage (Fig. 3a). This finding is in agreement with clinical studies showing that human heterozygous carriers of *SLC4A1* mutations can have hematopoietic abnormalities³³. These findings indicate that the many gene functions required to make embryonic erythrocytes are similarly required in their adult counterparts at full gene dosage for normal function.

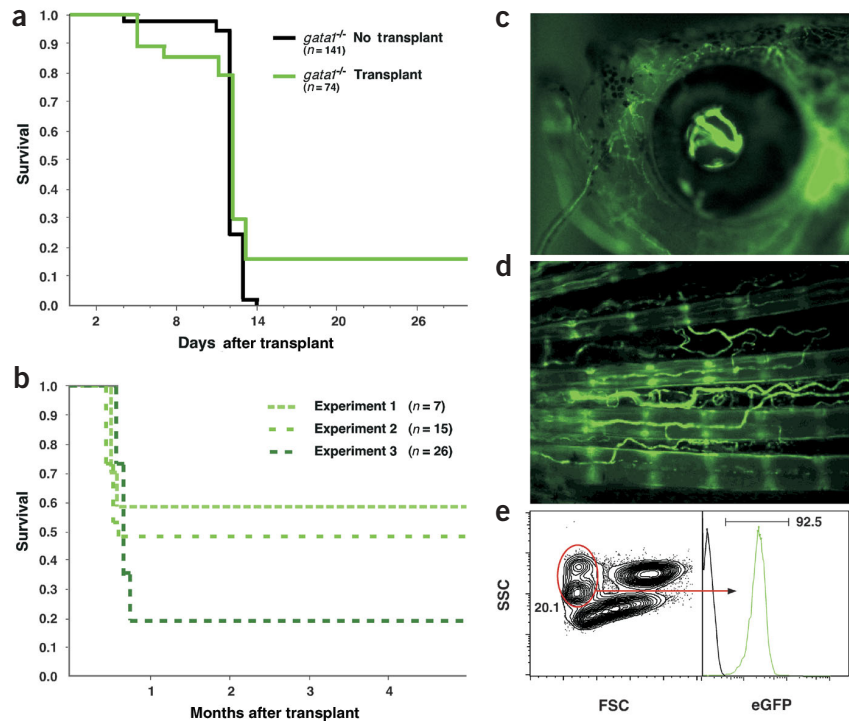
Occasional homozygous mutants can be raised to adulthood from certain lines, including merlot, retsina and pinotage¹³. Some of these mutant animals can survive for several months with an almost

complete absence of erythrocytes. For example, both *ebp41*^{-/-} and *slc4a1*^{-/-} adults had almost no cells in the erythroid scatter population (Fig. 3b,d). The precursor fraction in *ebp41*^{-/-} animals was increased more than ninefold compared with that of wild-type animals (Fig. 3d). Most cells in this fraction phenotypically resembled polychromatophilic erythroblasts (Fig. 3b). Adult *slc4a1*^{-/-} animals had a very similar phenotype, with a relative precursor increase of approximate eightfold compared with that of wild-type (Fig. 3d). The adult phenotypes of both *ebp41*^{-/-} and *slc4a1*^{-/-} mutants closely resembled their embryonic phenotypes, indicating that each gene has the same function in both primitive and definitive red blood cell production. The pinotage mutant, which has a mutation in an as-yet-unidentified gene, showed no heterozygous phenotype but was anemic and showed a considerable increase in erythroid precursors when homozygous (Fig. 3d). Among all mutants analyzed, we found no notable alterations reproducibly in the lymphoid or myeloid populations.

Hematopoietic cell transplantation rescues lethal *gata1*^{-/-} mutants

In mammals, transplantation has been used extensively to functionally test putative hematopoietic stem and progenitor cell populations, precursor-progeny relationships and cell autonomy of mutant gene function. To address similar issues, we developed hematopoietic cell transplantation in zebrafish. For a donor cell marker of transplanted cells, we used adult *gata1*^{eGFP} transgenic zebrafish. As zebrafish erythrocytes have lifespans limited to several weeks¹⁴, continued production of GFP⁺ cells over several months serves as a surrogate marker of stem and progenitor cell activity. We used transparent embryos 48 h after fertilization as transplant recipients to easily visualize donor-derived cells. These recipients are also optimal for the prevention of graft rejection, as the onset of lymphopoiesis does not occur until 3–5 d after fertilization^{34,35}. This is important, as it has not been possible to develop true inbred strains in zebrafish. We sought to determine whether transplantation could rescue otherwise lethal embryonic blood mutants. Both the moonshine (*mon/mon*)¹³ and vlad tepes (*gata1*^{-/-})^{14,36} blood mutants show a complete absence of erythroid cells and die by 14 days after fertilization. Transplantation of *gata1*^{eGFP} WKM into *mon/mon* mutants showed that donor-derived GFP⁺ cells homed to the pronephros and proliferated over a 10-day ‘window’ after

Figure 4 Hematopoietic cell transplantation rescues lethality in *gata1*^{-/-} mutants. **(a)** Kaplan-Meier survival curves of untransplanted versus transplanted homozygous *gata1*^{-/-} blood mutants. Untransplanted mutants do not survive past 14 d after fertilization, whereas transplantation of WKM rescues survival of approximately 20% of mutant recipients for at least 1 month. **(b)** Survival of transiently reconstituted *gata1*^{-/-} mutants. **(c,d)** A *gata1*^{-/-} transplant recipient at 8 weeks **(c)**; still image from **Supplementary Video 1** online) and 6 months **(d)** after transplantation. **(e)** Flow cytometry analysis of a *gata1*^{-/-} transplant recipient at 6 months after transplantation. All erythroid cells are GFP⁺ (green histogram, right).



transplantation to reach blood cell numbers similar to those of wild-type siblings. However, rescue of hematopoiesis failed to rescue mutant survival (D. Ransom, D.T. and L.I.Z., unpublished data). These findings indicate that moonshine acts in a cell-autonomous way in the generation of erythrocytes, but that nonhematopoietic defects also contribute to embryonic lethality.

Transplantation of the vlad tepes mutant, which results from a defect in *gata1* (ref. 36), showed rescue of both erythropoiesis and long-term survival (Fig. 4). Unlike the results obtained with untransplanted *gata1*^{-/-} mutants, transplantation of WKM into *gata1*^{-/-} mutants was sufficient to rescue approximately 20% of individual recipients (Fig. 4a). Three independent experiments in which we assigned scores to embryonic recipients for high-level reconstitution of GFP⁺ cells on day 2 after transplantation (between 1×10^2 and 1×10^3 GFP⁺ cells per animal) showed approximately 60%, 50% and 20% survival over several months (Fig. 4b). Most animals had circulating GFP⁺ cells at numbers indistinguishable from those of age-matched *gata1*^{eGFP} donors, as assessed by videomicroscopy (Fig. 4c,d and **Supplementary Video 1** online) for up to 8 months after transplant. In recipients killed at 6 months after transplant, all erythrocytes in WKM were donor derived, based on GFP expression (Fig. 4e).

Hematopoietic stem cells are in the lymphoid fraction

To assess which scatter fraction contains long-term HSCs, we transplanted each from *gata1*^{eGFP}-transgenic donors into wild-type embryos at 48 h after fertilization. We found GFP⁺ cells in the circulation 1 week after transplantation of the lymphoid, erythroid and precursor fractions (Table 2). At 5 weeks after transplantation, however, GFP⁺ cells were present only in lymphoid recipients. At 5 weeks, 5 of 110 original transplant recipients were GFP⁺; 2 of these continued to produce transgenic erythrocytes at 6 months after transplantation. These data indicate that the lymphoid fraction is the only population in WKM that contains cells capable of generating erythrocytes for more than 1 month. That GFP⁺ cells continue to be produced for over 6 months also indicates that the lymphoid fraction contains long-term reconstituting HSCs.

Visualization of multilineage engraftment in living recipients

The optical transparency of zebrafish embryos and larvae, combined with transgenic technology, provides an ideal system for studying blood cells in their natural environment. In the context of transplantation, we sought markers to independently label erythrocytes and

leukocytes to follow multilineage, donor-derived hematopoiesis and early trafficking events. Analysis of GFP in adult kidney cells isolated from zebrafish carrying a *bactin*^{eGFP} transgene showed that only leukocytes were GFP⁺ (Fig. 5a), with no expression above background detected in the erythrocyte fraction. GFP was expressed in approximately 97% of the myeloid fraction, 78% of the precursor fraction and 52% of the lymphoid fraction. To create a new marker of the erythroid lineage, we used the *gata1* promoter to create new germline transgenic animals expressing the dsRED fluorescent protein. Analysis of kidney scatter populations showed that approximately 93% of the erythroid fraction, 6% of the lymphoid fraction and 11% of the precursor fraction expressed the *gata1*^{dsRED} transgene. Expression in myeloid cells could not be detected above background fluorescence. As each of these promoters drives expression in nearly mutually exclusive subsets of blood cells, we generated double-transgenic animals for transplantation experiments. Transplantation of double-positive WKM into wild-type recipients at 48 h after fertilization showed GFP⁺ cells that trafficked to the developing thymus and pronephros, whereas dsRED⁺ cells were seen only in circulation (**Supplementary Video 2** online). Examination of recipients under high power showed two types of GFP⁺ cells that rolled along the endothelial surfaces of blood vessels. The first were small, round cells that rolled steadily along the vessels (Fig. 5b and **Supplementary Video 2** online), similar to the activity described for murine lymphocytes³⁷. The second were large, amoeboid cells with visible pseudopodia that moved along vessels by an end-over-end motion (Fig. 5b and **Supplementary Video 2** online), indicative of myelomonocytic cells. The latter type of cells invaded many tissues, and occasionally these cells were fluorescent in both the GFP and dsRED channels, possibly resulting from phagocytosis of donor-derived erythrocytes (data not shown).

As transplantation into wild-type animals results in competition for engraftment by host cells, we did similar transplants into *gata1*^{-/-} and bloodless mutant embryos. The bloodless mutation is dominant

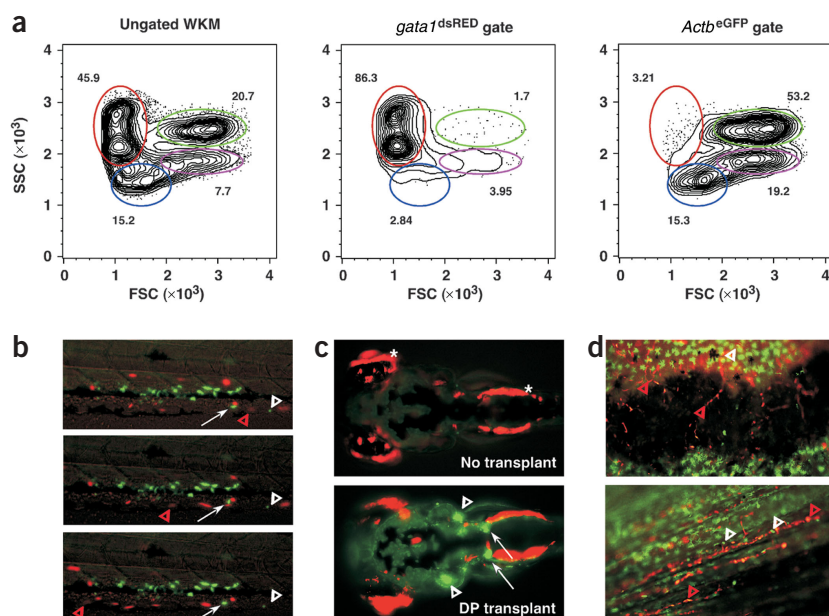
Table 2 Transplantation of kidney scatter populations from *gata1^{eGFP}* donors

Population	<i>n</i>	Number of GFP ⁺ recipients		
		1 Week	5 Weeks	6 Months
Lymphoid	110	15	5	2
Erythroid	40	11	0	0
Precursor	60	5	0	0
Myeloid	40	0	0	0

and partially penetrant, and embryos often show complete absence of primitive blood cells¹⁷. Definitive blood production is delayed but generally recovers by late larval stages. Whereas transplantation of *gata1^{-/-}* mutants resulted in robust reconstitution of dsRED⁺ erythrocytes, reconstitution of GFP⁺ leukocytes occurred at levels similar to those in wild-type recipients. Analysis of the developing thymus and pronephros in either *gata1^{-/-}* or wild-type recipients showed only low numbers of GFP⁺ leukocytes (data not shown). The *gata1^{-/-}* mutants transplanted with double-positive WKM survived for more than 8 weeks with continued production of both GFP⁺ and dsRED⁺ kidney cells (*n* = 16; data not shown), demonstrating multilineage reconstitution that probably resulted from HSCs contained in the graft. In contrast to *gata1^{-/-}* recipients, transplantation of double-positive WKM into bloodless hosts showed rapid and robust contribution of GFP⁺ cells to the developing thymus and pronephros (*n* = 13; Fig. 5c and Supplementary Video 3 online). Rapid expansion of dsRED⁺ cell populations occurred in bloodless recipients over the first week after transplantation (data not shown). The robust engraftment of double-positive WKM cells in embryonic bloodless recipients led to the continued proliferation of donor-derived cells into adulthood, indicating the endurance of donor HSC activity in bloodless recipients (*n* = 7; Fig. 5d and Supplementary Video 4 online).

Figure 5 Transplantation of WKM from double-transgenic donors allows independent visualization of leukocytes and erythrocytes in translucent recipient embryos. (a) Scatter profile of ungated WKM in a representative *gata1^{dsRED} bactin^{eGFP}* double-transgenic adult (left). The dsRED⁺ cells are only in the erythrocyte gate (middle), whereas GFP⁺ cells are nonerythroid (right). Numbers in plots indicate percent of cells in circled gate.

(b,c) Transplantation of recipients at 48 h after fertilization shows transient reconstitution of donor-derived erythrocytes and leukocytes. (b) Visualization of the tail vessels in a *gata1^{-/-}* transplant recipient shows a slow-moving, round leukocyte (white arrowheads), a larger leukocyte showing an end-over-end tumbling migration (arrows), and a rapidly circulating erythrocyte (red arrowheads) at 1 d after transplantation. Each frame is from Supplementary Video 2 online, and is separated by 300 ms (original magnification, ×20; anterior to the left). (c) Dorsal views comparing untransplanted (upper) and transplanted bloodless recipients (lower). The bloodless recipients show rapid and robust engraftment of the pronephros (arrows) and bilateral thymi (arrowheads) by GFP⁺ leukocytes by day 5 after transplantation. *, autofluorescence of the eyes and swim bladder in the dsRED channel. DP, double-positive. (d) The bloodless recipients show sustained, multilineage hematopoiesis from donor-derived cells. Top, robust reconstitution of dsRED⁺ erythrocytes (red arrowheads) and GFP⁺ leukocytes (white arrowhead) as seen in the dermal capillaries of a bloodless recipient at 8 weeks after transplantation. Bottom, similar multilineage reconstitution as seen in the tail capillaries of another bloodless recipient at 8 weeks (original magnification, ×20; still image from Supplementary Video 4 online).

**DISCUSSION**

Despite more than 450 million years of evolutionary divergence, hematopoiesis in teleosts is very similar to that in mammals. As reported here and elsewhere^{38–41}, definitive blood cell lineages in zebrafish show a high degree of conservation at the morphological level to their mammalian counterparts. Gene expression studies¹², functional studies^{23,25,41,42} and elucidation of mutant blood genes^{30–32,36} have indicated that the general mechanisms of hematopoietic development and effector cell functions are likewise conserved. These characteristics, combined with the potential of high-throughput genetic screens, make zebrafish unique vertebrates in which to study blood cell formation.

At present, however, there is a paucity of reagents available for the study of zebrafish blood cells. The ability to separate each hematopoietic lineage from others has been crucial in driving our understanding of mammalian hematopoiesis. By far the most important technology for lineal purification has been the production of monoclonal antibodies. Generation of monoclonal antibodies to the blood cells of nonmammalian vertebrates has been difficult, presumably because of differences in glycosylation patterns that are overwhelmingly recognized by the rodent immune system as foreign. Our attempts, as well as those of other investigators⁴³, to generate mouse monoclonal antibodies to teleost have mostly yielded nonspecific clones that uniformly label all leukocytes. Although attempts in catfish⁴⁴, carp^{45,46} and trout^{47,48} have had limited success in generating antileukocyte reagents, we have yet to obtain specific clones with zebrafish kidney marrow (D.T. A. Winzeler, J. Sullivan, J. DiCaprio and L. I. Z., unpublished data). It is therefore fortunate that the major hematopoietic lineages can be isolated to near purity by flow cytometry with only light-scatter characteristics. With this relatively simple technique, we have shown that scatter profiling yields similar results in all common zebrafish strains, and that aberrant populations, such as leukemic T lymphocytes, can be easily visualized

and purified to homogeneity for further genetic, morphologic and transplantation studies²⁸. We have also shown that the expression of lineage-affiliated genes in zebrafish transgenic lines correlate well with our lineal scatter populations. Transplantation of each scatter population has also shown HSC activity to be contained only in the lymphoid fraction, which will aid future HSC enrichment strategies. Flow cytometry-based lineage analyses should similarly prove useful in characterizing adult mutants identified in ongoing lymphoid, myeloid and stem cell mutagenesis screens.

We have demonstrated that many of the embryonic zebrafish blood mutants are anemic as adults, some even as heterozygous carriers of recessive mutations. Reductions in red cell numbers are consistently associated with apparently compensatory increases in erythroid precursors, which can be precisely counted and isolated with flow cytometry. Animals heterozygous for the *slc4a1* mutation, for example, have a phenotype intermediate to that of homozygous mutants and wild-type controls. This indicates that *slc4a1* is haploinsufficient when present in only one copy. Humans with only one functional copy of *SLC4A1* also show erythropoietic abnormalities³³, supporting our findings in the zebrafish and strengthening its utility as a faithful model of mammalian hematopoiesis. In contrast, heterozygous carriers of the *ebp41* mutation show no apparent defect. The *ebp41* gene encodes protein 4.1R³⁰, which physically interacts with SLC4A1 in the erythrocyte cytoskeleton⁴⁹. Why *slc4a1* mutants are not similarly haploinsufficient is unclear, but this may be because of redundant functions of closely related orthologs⁵⁰. Rare animals homozygous for mutations in either *slc4a1* or *ebp41r* that survive to adulthood show similar phenotypes, with few to no erythrocytes and huge increases in immature erythroid precursors. Cells resembling late basophilic erythroblasts are found in circulation in both mutants^{30,31}, and these may be sufficient for minimal oxygenation of adult tissues. Animals with heterozygous mutations in unknown genes, such as pinotage mutants, showed no notable phenotypic differences, but as homozygotes showed erythroid-specific defects similar to those of animals with mutations in *slc4a1* or *ebp41*. This may indicate that pinotage represents a mutation in a gene encoding another erythrocyte membrane protein. When candidate gene approaches are used to identify unknown mutated genes, flow cytometry-based profiling may thus be helpful in refining candidate choice to genes associated with similar mutant phenotypes.

We developed hematopoietic cell transplantation to provide means to test cell autonomy of mutant gene function, to test for leukemic transformation²⁸ and to establish a rigorous assay to test for HSC activity. As it has not been possible to create inbred zebrafish lines, allogeneic transplant rejection is an important concern. Transplantation of *gata1*^{eGFP} WKM into nontransgenic, adult siblings resulted in the disappearance of GFP⁺ cells in several weeks, indicating that donor cells are rejected by the host immune system. To lessen histocompatibility issues, we used embryonic recipients at 48 h after fertilization that had not yet developed lymphocyte subsets^{34,35,51}. Transplantation of transgenic cells in this setting led to the persistence of GFP⁺ cells for many months, indicating that hosts are tolerized to transplants when transplantation is done before the development of specific immunity. Although we cannot rule out the possibility of responses against host tissues by lymphocytes contained in transplanted WKM, we found no overt signs of graft-versus-host disease. We next studied hematopoietic cell transplantation in the context of mutant backgrounds, including moonshine, *gata1*^{-/-} and bloodless. As discussed above, transplantation into moonshine mutants led to transient and robust reconstitution of GFP⁺ blood cells that approached wild-type levels, yet failed to rescue embryonic lethality. This indicates that moonshine normally functions in a cell-autonomous way in blood cells, and that nonhematopoietic defects

contribute to lethality. Without transplantation, this issue would have been difficult to determine, as moonshine mutants die at approximately the same stage at which other mutants, such as *gata1*^{-/-} mutants, die because of erythropoietic failure. Given the results of targeted disruption of *Gata1* in the mouse⁵²⁻⁵⁴, zebrafish *gata1* should act in a cell-autonomous and blood-specific way. Hematopoietic cell transplantation with transgenic WKM indeed led to rescue of both hematopoiesis and long-term survival of *gata1*^{-/-} mutants for at least 6 months. This indicates that HSCs in donor WKM can stably engraft *gata1*^{-/-} mutants and provide long-term reconstitution of at least red blood cells. HSC frequency in the mouse has been estimated to be approximately 0.02–0.05% of cells within whole bone marrow^{1,2}. Assuming that HSC frequency is similar in the zebrafish kidney, we estimate that our transplantations with WKM were probably near limit dilution in terms of long-term reconstitution, as the maximum transplantable cell number is approximately 2×10^3 to 3×10^3 per embryo. If so, this would account for the relatively low percentage of long-term transplant survival (approximately 20%), and would indicate that long-term survival is mediated by engraftment of single or very few HSCs. Several long-term *gata1*^{-/-} transplant survivors (>6 months) gradually lost GFP⁺ erythrocytes until they became severely anemic and died (data not shown). These findings are very similar to those reported for transplantation of mouse c-Kit 'W' mutants⁵⁵. Transplantation of near limit-dilution doses of whole fetal liver suspensions into an allelic series of c-Kit mutants showed that engraftment efficiency positively correlated with increasing mutant severity, and that donor cells occasionally disappeared over time. In both mouse and zebrafish examples, we found no overt signs of graft-versus-host disease or graft rejection, indicating that this loss of engraftment is a normal activity of HSCs when they are transplanted in very limited numbers. Accordingly, studies in which highly purified, single HSCs were transplanted similarly showed many recipients lose engraftment over time^{3,56}. These data indicate that the *gata1*^{-/-} transplant model is sufficiently sensitive for near-limit-dilution transplants, and will provide an excellent system in which to test HSC enrichment strategies.

In the transplantation experiments described above, donor derivation was measured by continued production of GFP⁺ erythrocytes from a *gata1*^{eGFP} transgene. To mark both the erythroid and nonerythroid blood lineages, we subsequently transplanted cells with both *bactin*^{eGFP} and *gata1*^{dsRED} transgenes. Visualization of donor-derived cells over the first few days after transplantation showed dsRED⁺ cells were ovoid cells that circulated rapidly, whereas most GFP⁺ cells were found rolling along the lumens of blood vessels. We found two classes of rolling cells; their activity was indicative of each consisting of either lymphocytes or myelomonocytes. That both GFP⁺ cell types could be found morphologically in the developing thymus indicates that transplantation of wild-type marrow cells, or purified myeloid or lymphoid subsets, into lymphoid mutants¹⁸ may serve as a useful tool to determine whether thymic defects result from aberrant stromal elements or from defects intrinsic to T cell precursors. Transplantation into bloodless hosts resulted in more rapid and robust appearance of GFP⁺ cells in the developing thymus and pronephros. This is somewhat unexpected, as bloodless has been described to act non-cell autonomously¹⁷, indicating that the gene mutated in bloodless is required as an environmental factor. These non-cell-autonomous requirements, however, were assayed only for embryonic cell types. Although initially bloodless, these mutants later recover to produce all definitive cell subsets. Based on gene expression profiles, all definitive blood cell lineages are considerably delayed in their recovery to near wild-type levels. This observation, combined with our transplantation results with definitive cell types, indicates that bloodless animals may be ideal

recipients for hematopoietic cell transplantation by providing an environment that is relatively free of competing host cells over the first few days of development. This is also in agreement with findings in which increasing transplant engraftment efficiency was determined by available niche space in increasingly severe c-Kit mutant recipients⁵⁵. It will be useful to compare engraftment efficiency between *gata1*^{-/-} and bloodless recipients once HSC-enrichment methods become available.

The advent of assays in which both leukocytes and erythrocytes can be independently measured in unperturbed, *in vivo* environments provides a useful tool to study multilineage hematopoiesis from candidate HSC populations as well as homing of specific cell subsets to the thymus and pronephros, all of which can be visualized *in situ* in real time. This system is thus suitable for the study of HSC biology, and will serve as a model to test the enrichment of candidate, prospectively isolated HSC subsets from the zebrafish kidney, and to examine the functional defects of known and arising zebrafish blood mutants. With hematopoietic cell transplantation assays and future means to prospectively isolate HSCs, the zebrafish model will be positioned to elucidate the elusive genetics of HSC biology.

METHODS

Zebrafish. Zebrafish were mated, staged and raised as described⁵⁷ and were maintained in accordance with Animal Research at Children's Hospital guidelines. Blood mutants, including merlot³⁰, retsina³¹, riesling³², bloodless¹⁷, pinotage and moonshine¹³, and vlad tepe³⁶ were obtained from crosses of heterozygous parents and were assigned scores for hematopoietic defects from 2 to 4 days after fertilization.

Transgenic *gata1*^{dsRED} zebrafish were generated by subcloning of a 7-kb zebrafish *gata1* promoter fragment into the multiple cloning site of the pDsRed 2-1 vector (Clontech). The transgenic construct was excised using *XhoI* and *AflIII* and was isolated from the vector by electrophoresis and Qiaquick extraction (Qiagen). Purified DNA was resuspended to a concentration of 100 ng/μl in injection buffer containing 5 mM TrisHCl, 0.5 mM EDTA and 100 mM KCl, and was injected into zebrafish embryos at the one-cell stage of development. Animals with resulting transient expression were grouped and crossed to identify germline founders.

Zebrafish transgenic for *gata2*^{eGFP} were generated by insertion of a GFP reporter gene immediately downstream of the ATG start site in *gata2* bacterial artificial chromosome (BAC) constructs by Chi-mediated homologous recombination (W.T.P. and S.L., data not shown). The BAC-1 element used in these studies contained 70–80 kb of genomic zebrafish *gata2* DNA, which represents approximately 20.7 kb of promoter sequence upstream of the start site. Unlike *gata2* germline transgenics made with a 7.3-kb plasmid-based construct, transgenic embryos derived from the BAC-1 founder line have shown this construct faithfully recapitulates the endogenous expression of *gata2* in both neural and hematopoietic tissues (W.T.P. and S.L., data not shown). The gene encoding platelet glycoprotein IIb (integrin α_{IIb} ; gene name, *itga2b*) is found on contig 26,744 of the zebrafish genome array at the Sanger center (http://www.ensembl.org/Danio_rerio, and <http://134.174.23.160/CompGenomics/>). The *itga2b*^{eGFP} transgenic line was constructed with 6 kb of promoter linked to eGFP (H.F. Lin and R. Handin, unpublished data). The promoter was cloned from PAC 166I10. The *gata1*^{eGFP} and *rag2*^{eGFP} transgenic lines were generated as described^{28,29}. All experiments were done according to the guidelines of Animal Research at Children's Hospital.

Cell collection. Wild-type adult zebrafish were anaesthetized with 0.02% tricaine before blood, kidney and spleen collection. Blood was obtained by cardiac puncture with micropipette tips coated with heparin and was immediately smeared onto glass slides. After a ventral, midline incision was made, the spleen and kidney were dissected and placed into ice-cold 0.9× PBS containing 5% FCS. Single-cell suspensions were generated by aspiration followed by gentle 'teasing' of each organ on a 40-μm nylon mesh filter with a plunger from a 1-ml syringe.

Cytology. Cytospin preparations were made with 1×10^5 to 2×10^5 kidney cells or splenocytes cytocentrifuged at 300 r.p.m. for 3 min onto glass slides in a

Cytospin3 cytocentrifuge (Shandon). Blood smears and cytospin preparations were processed through May-Grünwald and Giemsa stains (Fluka) for morphological analyses and differential cell counts.

Flow cytometry. Hematopoietic cells isolated from wild-type or mutant zebrafish were processed as described above, washed and resuspended in ice-cold 0.9× PBS plus 5% FBS, and were passed through a filter with a 40-μm pore size. Propidium iodide (Sigma) was added to a concentration of 1 μg/ml to exclude dead cells and debris. Flow cytometry analysis and sorting was based on propidium iodide exclusion, forward scatter and side scatter, and GFP and/or dsRED fluorescence with a FACSVantage flow cytometer (Beckton Dickinson). Sorted cell populations were run twice to optimize cell purity. Flow cytometry differentials of prothrombocytes and thrombocytes were done with transgenic *itga2b*^{eGFP} fish (W.F. Lin, D.T., C. Abraham and R. Handin, unpublished data). Mean cell sizes of scatter populations were determined by linear normalization to 2-μm and 10-μm latex beads with forward scatter.

Hematopoietic cell transplantation. WKM cells (3×10^6 to 6×10^6) were isolated from adult transgenic donors as described above and were filtered and washed three times before a final resuspension in 10 μl 0.9× PBS containing 5% FCS. To lessen aggregation, 1 U DNaseI (Life Technologies) and 3 U heparin (Sigma) were added. Transplant recipients were anesthetized in tricaine and immobilized in individual conical wells made in 2% agarose. Approximately 1×10^2 to 1×10^3 kidney marrow cells were injected into the sinus venosus of wild-type and mutant embryos at 48 h after fertilization through borosilicate glass capillary needles (1 mm outside diameter, no filament; World Precision Instruments) made with a Flaming/Brown micropipette puller (Sutter Instruments). Cell suspensions were back-loaded into each needle and injected into circulation by forced air with a Narishige injection station and a Narashige micromanipulator. Recipient embryos were maintained in embryo medium containing penicillin and streptomycin during and for several hours after transplantation to prevent infection. Transplanted embryos were visualized daily with an inverted fluorescent microscope (Leica DM-IRE2) to monitor survival and GFP⁺ cells over a span of 7 d, after which larvae were introduced into our fish system. Imaging of transplant recipients was made with a Hammamatsu Orca-ER digital camera and Openlab software.

ACKNOWLEDGMENTS

We thank A. Kiger, N. Trede, and P. Ernst for critical evaluation of the manuscript; H. Stern, J. Amatruda, and M. Fleming for providing sections and review of histology; A. Flint and M. Handley for assistance with flow cytometry; and D. Langenau and T. Look, and H.F. Lin and R. Handin, for providing *rag2*^{eGFP} and *itga2b*^{eGFP} transgenic zebrafish, respectively, prior to publication. We thank R. Wingert and J. Cope for providing mutant lines; H. Zhu for assistance with the *gata1*^{dsRED} line; and A. Winzeler for technical assistance. Supported by the Irving Institute for Immunological Research (D.T.); the Howard Hughes Medical Institute (B.P. and L.I.Z.); the National Institutes of Health (B.P. and L.I.Z.) and the William Randolph Hearst Foundation (B.P.); and the Grousbeck family and Legal Sea Foods (L.I.Z.).

Note: Supplementary information is available on the Nature Immunology website.

COMPETING INTERESTS STATEMENT

The authors declare that they have no competing financial interests.

Received 17 June; accepted 14 October 2003

Published online at <http://www.nature.com/natureimmunology/>

- Spangrude, G.J., Heimfeld, S. & Weissman, I.L. Purification and characterization of mouse hematopoietic stem cells. *Science* **241**, 58–62 (1988).
- Morrison, S.J. & Weissman, I.L. The long-term repopulating subset of hematopoietic stem cells is deterministic and isolatable by phenotype. *Immunity* **1**, 661–673 (1994).
- Osawa, M., Hanada, K., Hamada, H. & Nakauchi, H. Long-term lymphohematopoietic reconstitution by a single CD34-low/negative hematopoietic stem cell. *Science* **273**, 242–245 (1996).
- Kondo, M., Weissman, I.L. & Akashi, K. Identification of clonogenic common lymphoid progenitors in mouse bone marrow. *Cell* **91**, 661–672 (1997).
- Akashi, K., Traver, D., Miyamoto, T. & Weissman, I.L. A clonogenic common myeloid progenitor that gives rise to all myeloid lineages. *Nature* **404**, 193–197 (2000).
- Shivdasani, R.A., Mayer, E.L. & Orkin, S.H. Absence of blood formation in mice lacking the T-cell leukaemia oncprotein tal-1/SCL. *Nature* **373**, 432–434 (1995).
- Yamada, Y. *et al.* The T cell leukemia LIM protein Lmo2 is necessary for adult mouse

- hematopoiesis. *Proc. Natl. Acad. Sci. USA* **95**, 3890–3895 (1998).
8. Warren, A.J. *et al.* The oncogenic cysteine-rich LIM domain protein rbtn2 is essential for erythroid development. *Cell* **78**, 45–57 (1994).
 9. Okuda, T., van Deursen, J., Hiebert, S.W., Grosfeld, G. & Downing, J.R. AML1, the target of multiple chromosomal translocations in human leukemia, is essential for normal fetal liver hematopoiesis. *Cell* **84**, 321–330 (1996).
 10. Mucenski, M.L. *et al.* A functional c-myc gene is required for normal murine fetal hepatic hematopoiesis. *Cell* **65**, 677–689 (1991).
 11. Ivanova, N.B. *et al.* A stem cell molecular signature. *Science* **298**, 601–604 (2002).
 12. Amatruda, J.F. & Zon, L.I. Dissecting hematopoiesis and disease using the zebrafish. *Dev. Biol.* **216**, 1–15 (1999).
 13. Ransom, D.G. *et al.* Characterization of zebrafish mutants with defects in embryonic hematopoiesis. *Development* **123**, 311–319 (1996).
 14. Weinstein, B.M. *et al.* Hematopoietic mutations in the zebrafish. *Development* **123**, 303–309 (1996).
 15. Liao, E.C. *et al.* SCL/Tal-1 transcription factor acts downstream of cloche to specify hematopoietic and vascular progenitors in zebrafish. *Genes Dev.* **12**, 621–626 (1998).
 16. Parker, L. & Stainier, D.Y. Cell-autonomous and non-autonomous requirements for the zebrafish gene cloche in hematopoiesis. *Development* **126**, 2643–2651 (1999).
 17. Liao, E.C. *et al.* Non-cell autonomous requirement for the bloodless gene in primitive hematopoiesis of zebrafish. *Development* **129**, 649–659 (2002).
 18. Trede, N.S., Zapata, A. & Zon, L.I. Fishing for lymphoid genes. *Trends Immunol.* **22**, 302–307 (2001).
 19. Herbomel, P., Thisse, B. & Thisse, C. Zebrafish early macrophages colonize cephalic mesenchyme and developing brain, retina, and epidermis through a M-CSF receptor-dependent invasive process. *Dev. Biol.* **238**, 274–288 (2001).
 20. Traver, D. & Zon, L.I. Walking the walk: migration and other common themes in blood and vascular development. *Cell* **108**, 731–734 (2002).
 21. Thompson, M.A. *et al.* The cloche and spadetail genes differentially affect hematopoiesis and vasculogenesis. *Dev. Biol.* **197**, 248–269 (1998).
 22. Burns, C.E. *et al.* Isolation and characterization of runxa and runxb, zebrafish members of the runt family of transcriptional regulators. *Exp. Hematol.* **30**, 1381–1389 (2002).
 23. Kalev-Zylinska, M.L. *et al.* Runx1 is required for zebrafish blood and vessel development and expression of a human RUNX1-CBF2T1 transgene advances a model for studies of leukemogenesis. *Development* **129**, 2015–2030 (2002).
 24. Zapata, A. Ultrastructural study of the teleost fish kidney. *Dev. Comp. Immunol.* **3**, 55–65 (1979).
 25. Jagadeeswaran, P., Sheehan, J.P., Craig, F.E. & Troyer, D. Identification and characterization of zebrafish thrombocytes. *Br. J. Haematol.* **107**, 731–738 (1999).
 26. Shapiro, H.M. Parameters and probes. In *Practical Flow Cytometry* 271–410 (Wiley-Liss, New York, 2002).
 27. Zon, L.I. *et al.* Expression of mRNA for the GATA-binding proteins in human eosinophils and basophils: potential role in gene transcription. *Blood* **81**, 3234–3241 (1993).
 28. Langenau, D.M. *et al.* Myc-induced T-cell leukemia in transgenic zebrafish. *Science* **299**, 887–890 (2003).
 29. Long, Q. *et al.* GATA-1 expression pattern can be recapitulated in living transgenic zebrafish using GFP reporter gene. *Development* **124**, 4105–4111 (1997).
 30. Shafizadeh, E. *et al.* Characterization of zebrafish merlot/chablis as non-mammalian vertebrate models for severe congenital anemia due to protein 4.1 deficiency. *Development* **129**, 4359–4370 (2002).
 31. Paw, B.H. *et al.* Cell-specific mitotic defect and dyserythropoiesis associated with erythroid band 3 deficiency. *Nat. Genet.* **34**, 59–64 (2003).
 32. Liao, E.C. *et al.* Hereditary spherocytosis in zebrafish riesling illustrates evolution of erythroid β -spectrin structure, and function in red cell morphogenesis and membrane stability. *Development* **127**, 5123–5132 (2000).
 33. Tanner, M.J. Band 3 anion exchanger and its involvement in erythrocyte and kidney disorders. *Curr. Opin. Hematol.* **9**, 133–139 (2002).
 34. Trede, N.S. & Zon, L.I. Development of T-cells during fish embryogenesis. *Dev. Comp. Immunol.* **22**, 253–263 (1998).
 35. Willett, C.E., Zapata, A.G., Hopkins, N. & Steiner, L.A. Expression of zebrafish rag genes during early development identifies the thymus. *Dev. Biol.* **182**, 331–341 (1997).
 36. Lyons, S.E. *et al.* A nonsense mutation in zebrafish gata1 causes the bloodless phenotype in vlad tepes. *Proc. Natl. Acad. Sci. USA* **99**, 5454–5459 (2002).
 37. Butcher, E.C. Leukocyte-endothelial cell recognition: three (or more) steps to specificity and diversity. *Cell* **67**, 1033–1036 (1991).
 38. Al-Adhami, M.A. & Kunz, Y.W. Ontogenesis of haematopoietic sites in *Brachydanio rerio*. *Dev. Growth Differ.* **19**, 171–179 (1977).
 39. Willett, C.E., Cortes, A., Zuasti, A. & Zapata, A.G. Early hematopoiesis and developing lymphoid organs in the zebrafish. *Dev. Dyn.* **214**, 323–336 (1999).
 40. Bennett, C.M. *et al.* Myelopoiesis in the zebrafish, *Danio rerio*. *Blood* **98**, 643–651 (2001).
 41. Lieschke, G.J., Oates, A.C., Crowhurst, M.O., Ward, A.C. & Layton, J.E. Morphologic and functional characterization of granulocytes and macrophages in embryonic and adult zebrafish. *Blood* **98**, 3087–3096 (2001).
 42. Herbomel, P., Thisse, B. & Thisse, C. Ontogeny and behaviour of early macrophages in the zebrafish embryo. *Development* **126**, 3735–3745 (1999).
 43. Bowden, L.A. *et al.* Generation and characterisation of monoclonal antibodies against rainbow trout, *Oncorhynchus mykiss*, leucocytes. *Comp. Biochem. Physiol. C Pharmacol. Toxicol. Endocrinol.* **117**, 291–298 (1997).
 44. Miller, N. *et al.* Functional and molecular characterization of teleost leukocytes. *Immunol. Rev.* **166**, 187–197 (1998).
 45. Secombes, C.J., van Groningen, J.J. & Egberts, E. Separation of lymphocyte subpopulations in carp *Cyprinus carpio* L. by monoclonal antibodies: immunohistochemical studies. *Immunology* **48**, 165–175 (1983).
 46. Rombout, J.H., Taverne-Thiele, A.J. & Villena, M.I. The gut-associated lymphoid tissue (GALT) of carp (*Cyprinus carpio* L.): an immunocytochemical analysis. *Dev. Comp. Immunol.* **17**, 55–66 (1993).
 47. Slierendrecht, W.J., Lorenzen, N., Glamann, J., Koch, C. & Rombout, J.H. Immunocytochemical analysis of a monoclonal antibody specific for rainbow trout (*Oncorhynchus mykiss*) granulocytes and thrombocytes. *Vet. Immunol. Immunopathol.* **46**, 349–360 (1995).
 48. Kollner, B., Blohm, U., Kotterba, G. & Fischer, U. A monoclonal antibody recognising a surface marker on rainbow trout (*Oncorhynchus mykiss*) monocytes. *Fish Shellfish Immunol.* **11**, 127–142 (2001).
 49. Lux, S.E. and Palek, J. Disorders of the red cell membrane. In *Blood: Principles and Practice of Hematology* (eds. Handin, R.I., Lux, S.E. & Stossel, T.P.) 1701–1818 (J.P. Lippincott, Philadelphia, 1995).
 50. Hoover, K.B. & Bryant, P.J. The genetics of the protein 4.1 family: organizers of the membrane and cytoskeleton. *Curr. Opin. Cell Biol.* **12**, 229–234 (2000).
 51. Danilova, N. & Steiner, L.A. B cells develop in the zebrafish pancreas. *Proc. Natl. Acad. Sci. USA* **99**, 13711–13716 (2002).
 52. Pevny, L. *et al.* Erythroid differentiation in chimaeric mice blocked by a targeted mutation in the gene for transcription factor GATA-1. *Nature* **349**, 257–260 (1991).
 53. Weiss, M.J., Keller, G. & Orkin, S.H. Novel insights into erythroid development revealed through in vitro differentiation of GATA-1 embryonic stem cells. *Genes Dev.* **8**, 1184–1197 (1994).
 54. Fujiwara, Y., Browne, C.P., Cunniff, K., Goff, S.C. & Orkin, S.H. Arrested development of embryonic red cell precursors in mouse embryos lacking transcription factor GATA-1. *Proc. Natl. Acad. Sci. USA* **93**, 12355–12358 (1996).
 55. Fleischman, R.A., Custer, R.P. & Mintz, B. Totipotent hematopoietic stem cells: normal self-renewal and differentiation after transplantation between mouse fetuses. *Cell* **30**, 351–359 (1982).
 56. Wagers, A.J., Sherwood, R.I., Christensen, J.L. & Weissman, I.L. Little evidence for developmental plasticity of adult hematopoietic stem cells. *Science* **297**, 2256–2259 (2002).
 57. Westerfield, M. *The Zebrafish Book: A Guide for the Laboratory Use of Zebrafish (Brachydanio rerio)* (University of Oregon Press, Eugene, 1994).